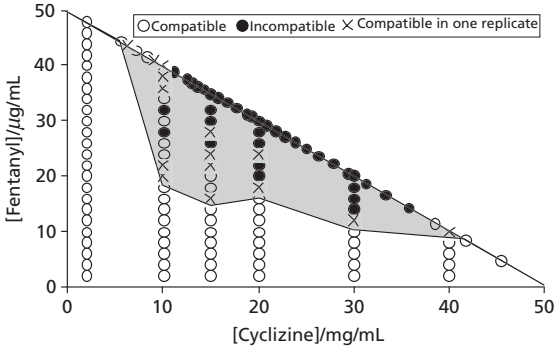

Figure 1 Compatibility of fentanyl citrate and cyclizine lactate injections at 25°C; duration = 2 hours. The shaded area indicates incompatible combinations.

precipitate was identified as cyclizine hydrochloride due to the presence of NaCl in the fentanyl injection.

Conclusions Physical compatibility boundaries for the mixtures were determined from the plate reader assay. In-syringe compatibility at 10 mg/mL cyclizine was in good agreement with the predicted compatibility.

80
Simultaneous estimation of lamivudine and zidovudine by reversed-phase high-performance liquid chromatography in tablet dosage forms

V. Karne, A. Wankhede, S. S. Patil and C. S. Magdum

Appasaheb Birnale College of Pharmacy, Sangli, Maharastra, India.
E-mail: vikramkarne@gmail.com

Objectives There are several UV, reversed-phase high-performance liquid chromatography (HPLC) and high-performance thin-layer chromatography methods available for simultaneous estimation of the drugs lamivudine and zidovudine but two reported methods can be used for simple, precise and fast simultaneous estimation of these drugs.

Methods Two simple, fast and precise reversed-phase HPLC methods have been developed and validated for the simultaneous estimation of lamivudine and zidovudine from tablet dosage forms. Lamivudine ((2*R-cis*)-4-amino-1-(2-(hydroxymethyl)-1,3-oxathiolan-5-yl)-2(1H)-pyrimidinone) and zidovudine (3′-azido-3′-deoxythymidine) are well-established anti-HIV agents. Lamivudine is official in Indian Pharmacopoeia [1] and [2] and zidovudine is official in Indian Pharmacopoeia [3] and [4]. In the first method the analytes were resolved by using a mixture of buffer (sodium phosphate)/acetonitrile/isopropyl alcohol (85:10:5, by vol.) as the mobile phase on a C_{18} column as a stationary phase and UV 277 nm as the detection wavelength. The retention times of lamivudine and zidovudine were 3–4 and 6–8 minutes respectively. In the second method the analytes were resolved by using a mobile phase of potassium dihydrogen phosphate/acetonitrile/isopropyl alcohol (85:10:5, by vol.) on a C_{18} column as a stationary phase and UV 277 nm as the detection wavelength. The retention times of lamivudine and zidovudine were 3–4 and 7–8 minutes respectively. No spectral or chromatographic interference from the tablet excipients was found.

Results The calibration plot was found to be linear and obeyed the Beer–Lambert law. Both methods were validated for precision, accuracy, linearity, reproducibility and robustness. Both methods were statistically compared by analysis of variance.

Conclusions The proposed two methods can suitably be applied to the assay of commercial formulations and used for routine quality-control applications.

Biopharmaceutics

81
Expedited solid-phase synthesis and utilization of affinity-based probes for the serine proteases

B. F. Gilmore and B. Walker

School of Pharmacy, Queen's University, Belfast, UK. E-mail: b.gilmore@qub.ac.uk

Objectives Serine proteases are one of the most widely studied classes of enzymes; this is largely due to their well-characterized, widespread and diverse roles in a host of physiological and pathological processes. Many pathological disorders are caused by a dysfunction in the normally exquisite regulation of the activity of these proteolytic enzymes, resulting in abnormal tissue destruction and/or the aberrant processing of other proteins and peptides. For example, serine proteases play a critical role in a number of processes, including extracellular matrix remodelling, angiogenesis, wound healing, tumour invasion and metastasis. We and others have previously reported on the synthesis and biochemical testing of peptides and amino acid analogues of amino alkyl diphenyl phosphonates as inhibitors of the serine proteases. These inhibitors exhibit an absolute selectivity of action for the serine protease class and function as time-dependent irreversible inhibitors of their target proteinases. We now wish to report on a novel expedited solid-phase synthesis approach for the generation of active-site-directed affinity probes based upon simple aminoalkyl diphenyl phosphonates and their application for the profiling and characterization of serine proteases obtained from a broad variety of bacterial, human and recombinant sources.

Methods The synthetic scheme employs recently available NovaTag™ resin technology that enables the facile synthesis of activity probes bearing fluorescent or biotin tags and which can also incorporate pegylated spacer units, if desired. Using this approach, we have synthesized a number of affinity probes that target serine proteases with differing P1 specificities. These probes are then used to detect, via affinity-based capture, serine protease activity in various biological milieux by standard electrophoresis and western-blotting techniques employing streptavidin-HP and a chemiluminescent substrate.

Results These inhibitors are potent, selective irreversible inhibitors of trypsin-, chymotrypsin- and elastase-like serine proteases. For example, the affinity-based probe biotin-PEG-succinyl-$Lys^{P}(OPh)_2$ had an overall second-order rate constant of 0.86×10^6 M^{-1} min^{-1}. The second-order rate constant for the inactivation of 4-hydroxy-2-nonenal (HNE) by biotin-PEG-succinyl-$Val^{P}(OPh)_2$ was determined to be 1.29×10^4 M^{-1} min^{-1}. The probes were used to disclose the activity of various serine proteases from both recombinant expression systems and from a range of biological samples including bacterial, mammalian and clinical (colonoscopy) samples. These probes have thus far been utilized to detect elevated levels of proteolytic activity from bacterial pathogens, inflammatory diseases of the colon and a variety of mammalian cells. The detected proteases can then be identified via exploitation of their interaction with immobilized streptavidin, and subsequent *de novo* sequencing, using mass spectrometry.

Conclusions This study reports the rapid, facile synthesis of a range of selective, potent, affinity-based probes for the serine proteases. The utility of these probes has been demonstrated in a number of examples presented. The probes will also find utility in the detection of proteases in numerous processes, especially chonic diseases where serine protease activities can be correlated with disease stage and progression.

82
Does reduced dissolution of paracetamol contribute to delayed absorption following single 60 and 90 mg/kg doses in third molar extractions?

N. J. Medlicott[1], K. Rizi[1,2], L. Yang[1], M. Zacharias[1,3], R. K. DeSilva[1] and D. M. Reith[1,3]

[1]University of Otago, Dunedin, New Zealand, [2]University of Bath, Bath, UK and [3]Otago District Health Board, Dunedin, New Zealand.
E-mail: natalie.medlicott@otago.ac.nz

Objectives To investigate paracetamol dissolution using a limited-volume US Pharmacopoeia (USP) dissolution test, then to investigate paracetamol plasma concentration time profiles following 60 and 90 mg/kg doses to determine whether limited solubility may influence paracetamol absorption in a clinical trial (Zacharias et al 2007).

Methods Paracetamol capsules were prepared (500 and 600 mg) in vegetable starch capsules (Wagner Pro-Biotics, Australia) and dissolution was compared with Panadol® caplets in a standard USP dissolution test. Dissolution media volume was reduced to 250 mL and dissolution of one, five, 10 and 15 capsules of 600 mg was determined at 37°C. Dissolution of 10 and 15 capsules was also determined in 250 mL 0.05 M HCl/0.25% w/v sodium dodecyl sulphate. Paracetamol dissolved was determined by UV spectroscopy (242 nm). In the clinical study, 600 mg capsules were administered pre-operatively for third molar extraction at 60 and 90 mg/kg in a randomized, double-blind cross-over study. Plasma was analysed for paracetamol at 0, 0.25, 0.5, 1, 1.5, 2, 3, 4, 8 and 24 hours by reversed-phase high-performance liquid chromatography.

Results USP dissolution test showed 80.6 ± 4.8, 79.4 ± 4.3 and 93.3 ± 3.2% dissolution in 45 minutes from 600 and 500 mg capsules and Panadol caplets respectively (n = 3). In 250 mL water, the percentage dissolved at 45 minutes was 76.5 ± 3.5, 72.1 ± 2.8, 55.6 ± 1.4 and 43.2 ± 3.0% for one, five, 10 and 15 capsules respectively. In simulated gastric fluid, the dissolution rate was lower, with 27.0 ± 4.5 and 26.5 ± 2.2% dissolved at 45 minutes for 10 and

Table 1 Paracetamol absorption parameters (mean ± SD)

	60 mg/kg	90 mg/kg
Absorption time lag (hour)	0.53 ± 0.43	0.86 ± 0.63
k_{abs} (hour^{-1})	2.5 ± 4.5	3.6 ± 3.8
T_{max} (hour)	2.75 ± 1.4	2.45 ± 1.2
Paracetamol dose/water ingested (mg/mL)	24 ± 10	38 ± 14

15 capsules respectively. Patients (n = 20) received 3–6 g (60 mg/kg) and 4.8–7.8 g (90 mg/kg) paracetamol as a single dose. The amount of water ingested with capsules was 80–360 mL (mean 189 ± 72 mL) and did not differ significantly between groups. A one-compartment pharmacokinetic model, first-order absorption and elimination with absorption time lag was fitted to the plasma concentration-time profiles. Absorption time lag (t_{lag}), rate (k_{abs}) and T_{max} were not significantly different between the two groups (Table 1; $P > 0.05$). At the 60 mg/kg dose, sufficient water was consumed with the capsules to dissolve the paracetamol (aqueous solubility, 20 mg/mL at 37°C; Shaw et al 2005). Paracetamol solubility was exceeded for the 90 mg/kg dose, but this did not appear to have greatly influenced the absorption pharmacokinetics of paracetamol. Correlation between paracetamol dose/water volume ingested and the absorption time lag was 0.276 ($P = 0.098$), suggesting only weak association.

Conclusions *In vitro* dissolution of paracetamol decreased in a limited-volume USP dissolution test with increasing numbers of capsules. However, reduced dissolution did not appear to significantly contribute to absorption lag time of paracetamol *in vivo*.

Shaw, L. R. et al (2005) *Drug Dev. Indust. Pharm.* **31**: 515–525
Zacharias, V. et al (2007) *Anaes. Intensive Care* **35**: 544–549

83
Freeze-drying cycle optimization for speed and protection using a liposome model

A. J. Ingham

University of Wolverhampton, Wolverhampton, UK. E-mail: a.j.ingham@wlv.ac.uk

Objectives To tackle the size-altering effects of freeze drying liposomes several approaches have been developed, including methods that do not involve drying at all. The most common approach, however, is the addition of a lyoprotectant to stabilize the structure and activity of the liposomes. Using a shelf-top temperature-controlled freeze dryer (Virtis adv) a liposome model was used to investigate lyophilization cycle design and the affect of sugars on protection during both poorly designed and optimized lyophilization cycles.

Methods Egg phosphatidylcholine (EPC) was rehydrated (7.8 mg/mL) from a thin film containing cholesterol (EPC/cholesterol, 16:8) to produce multilamellar vesicles. This colloid was then extruded to form large unilamellar vesicles of 1 μm, before the addition of various concentrations of sugars. Liposomes were then incubated at room temperature for 30 minutes and sized using laser light scattering. Freeze drying was then conducted in different cycle conditions which included: (a) slow cooling with high primary drying temperature (SH), (b) simulation of an uncontrolled shelf temperature or ambient temperature (AT), (c) annealing stage with low primary drying temperature (AL), (d) slow cooling with low primary drying temperature (SL) and (e) fast cooling with low primary drying temperature (FL).

Results The addition of the sugar lyoprotectants sucrose, trehalose and mannitol, and two less common potential protectants, raffinalose and melezitose (both trisaccharide sugars), was examined. A direct relationship was demonstrated between increasing sugar concentrations and a reduction in the size increase after freeze drying (a protection of liposome size). The most effective sugar at 125 mM was trehalose (FL). Poor performance was demonstrated by the crystallizing sugar mannitol in all cases with particularly poor performance in cycle AL, which was predicted: its ability to induce crystallization within the product was the likely cause. The freeze-drying cycle FL was able to provide protection equivalent to a size change from 1 μm (pre-freeze drying) to 19 μm (post-freeze drying) and with addition of sucrose (125 mM) 3.5 μm (post-freeze drying).

Conclusions Freeze-drying cycle design has been shown to be essential to particle-size protection of liposome populations, an important property in the targeting mechanism of this delivery vehicle. Unfortunately the most effective cycle (FL) for protection is also the longest and involves the lowest temperatures, making it the least economically viable. This suggests an economic role for freeze-drying optimization as well as an essential role in protecting the delivery vehicle during storage.

84
A 3Rs model consisting of a flow chamber and cells grown on a Transwell® membrane to mimic tissues and characterize delivery of novel medicines as a function of flow

H. Mcglynn[1], S. Lelu[1], C. Rauch[2], J. Penny[1] and A. Pluen[1]

[1]School of Pharmacy and Pharmaceutical Sciences, University of Manchester, Manchester and [2]School of Veterinary Medicine and Science, University of Nottingham, Nottingham, UK. E-mail: sylvie_lelu@yahoo.fr

Objectives Developing new medicines able to achieve specific targeting and to overcome cellular barriers has received considerable attention. However, assessing their delivery may either be performed *in vivo* or involve cells grown as monolayers. Unfortunately the latter approach might not reflect cellular behaviour *in vivo* (Abbot 2003). Indeed, recent studies have shown that the behaviour of vascular endothelial cells under shear stress differed when co-cultured with smooth muscle cells (Chiu et al 2003) and cells grown in spheroids show increased production of extracellular matrix and factors. Hence an efficient prediction of delivery rates requires the development of a system taking into account not only drug penetration through the cell membrane but also cell–cell interactions and parameters reflecting the cellular environment. The purpose of this study was to predict macromolecule delivery rates to endothelial cells by (1) mimicking blood flow through capillaries and the lymph drainage using a specifically designed flow chamber and (2) by taking into account cell–cell interactions through coculture of endothelial cells and human colon adenocarcinoma cells.

Methods Bovine endothelial cells (BAECs) and human colon adenocarcinoma Caco2 cells were cultured in eight-well plates and on the basal and apical surfaces of a Transwell® membrane (Fisher Scientific, Loughborough, UK). The Transwell® was then inserted into a flow chamber, the design of which allows the application of flow controlled by a syringe pump (Harvard pico 22) through the Transwell® membrane and in parallel with the membrane. Drug-delivery rates through cell membranes were measured using fluorescence correlation spectroscopy (FCS) at 633 nm on an inverted LSM 510 Meta-Confocor 2 (Carl Zeiss, Germany).

Results After optimizing concentrations, laser power, bleaching and measurement times were optimized, calcein diffusion times were measured in eight-well plates and in the flow chamber, giving diffusion times equal to 115 μs and around 130 μs respectively. FCS measurements of calcein diffusion times in BAECs and Caco2 cells grown in eight-well plates gave diffusion times between 300 and 2000 μs. The stability of the Transwell® membrane, and thus the ability to measure diffusion in cells, was assessed by recording the amplitude of the membrane vibrations. Typical vibration amplitudes of around 0.5 μm were measured, allowing FCS measurements in cells. Analysis of the correlation curve with an abnormal diffusion model indicates diffusion time between 200 and 1500 μs for calcein in Caco2 cells under a flow rate equal to 2 mL/h.

Conclusions The measurements validate the flow chamber/Transwell® system, strongly suggesting that novel medicines delivery to cells under flow is feasible. Further experiments will aim to measure the diffusion time of larger macromolecules such as BSA 647 and IgG 647 in cells as a function of the flow rate applied. Future plans also include increasing the system complexity by co-culturing BAECs and Caco2 cells on the lower and upper side of the Transwell® membrane respectively.

Abbot A. (2003) *Nature* **424**: 870–872
Chiu, J. J. et al (2003) *Blood Hemost Thrombosis Vasc Biol* **101**: 2667–2674

85
Manufacture and biopharmaceutical properties of co-crystals

M. Eigbire[1], B. Forbes[1] and C. Towler[2]

[1]King's College London, London and [2]Novartis Pharmaceuticals UK, Horsham, UK. E-mail: ben.forbes@kcl.ac.uk

Objectives Crystalline forms of active pharmaceutical ingredients (APIs) have traditionally been limited to salts, polymorphs and solvates (including hydrates). A new broad class of materials known as co-crystals offer better opportunities in terms of intellectual property and manipulation of biopharmaceutical performance (Vishweshwar et al 2006, Trask 2007). The aim of this study was to evaluate the potential to form co-crystals via manual and high-throughput methods. This was done by reproducing, from the literature, co-crystal formation with nicotinamide and cinnamic acid (1:1) and extending this to succinic, fumaric, oxalic, benzoic, maleic and malonic acid co-crystals. The same co-crystals were also made with benzamide. The biopharmaceutical properties (solubility and dissolution) of the co-crystal products were also evaluated.

Methods The samples were manufactured via slow evaporation from methanol solution and X-ray powder diffraction (XRPD) and differential scanning calorimetry (DSC) techniques were used to determine whether co-crystals had

been formed. The resulting co-crystals were subjected to standard dissolution and solubility testing. High-throughput methods were also used to make these co-crystals at differing ratios (including the ratio of the manually produced crystal), for comparison and to explore their potential for co-crystal manufacture.

Results DSC and XRPD analysis confirmed that co-crystals were formed, except with the combination of nicotinamide and benzamide with fumaric acid. Dissolution tests indicated that benzamide co-crystals (unlike nicotinamide co-crystals) had an enhanced dissolution profile compared with the pure API, although the solubility of nicotinamide and benzamide in co-crystal form was unchanged. Finally, high-throughput methods were found to produce co-crystals at the differing ratios, including the same co-crystals that were produced by the manual method.

Conclusions This study has demonstrated that co-crystals can be made manually and via high-throughput methods, and can offer opportunities for modification of biopharmaceutical properties such as dissolution rate. This raises the potential to enhance the bioavailability of active pharmaceutical ingredients.

Trask, A. V. (2007) *Mol. Pharm.* **4**: 301–309
Vishweshwar, P. et al (2006) *J. Pharm. Sci.* **95**: 499–516

Chemistry

86
Prediction of carcinogenicity of diverse chemical substances by a support vector machine

K. Tanabe[1] and T. Suzuki[2]

[1]University of Tsukuba, Tsukuba and [2]Toyo University, Tokyo, Japan.
E-mail: azul@oak.ocn.ne.jp

Objectives The ability to assess the toxicity of a chemical depends on the available information on the compound and/or its related compounds. Among chemicals currently in commerce, very few are ascertained on their toxicity, and reliable data on the carcinogenicity are very limited, especially for pharmaceutical chemicals. Therefore, attempts on the basis of quantitative structure–activity relationship (QSAR) models for estimating carcinogenicity have been performed (Benigni 2003, Tanabe et al 2005). The support vector machine (SVM) technique (Chen et al 2004) was applied to develop a QSAR model that relates the structures of diverse chemicals to their carcinogenicity in this study. Compared with traditional regression and neural network methods, SVMs have some advantages, including global optimum, good generalization ability and simple implementation.

Methods The carcinogenicity dataset used in the Predictive Toxicology Challenge 2000–2001 contest (Helma et al, http://www.informatik.uni-freiburg.de/~ml/ptc/) on 454 diverse chemicals was employed to develop the SVM model to compare its predictability with that of our previous artificial neural network (ANN) model (Tanabe et al 2005). The chemical carcinogenicity data consist of two discrete values (carcinogenic or non-carcinogenic). For the SVM modelling, LIBSVM ver.2.85 software (Chang and Lin, http://www.csie.ntu.edu.tw/~cjlin/libsvm/) was used for regression. Molecular descriptors calculated from the three-dimensional geometries of the compounds alone with Fujitsu Project-Leader were used to represent the molecules.

Results The relationship between experimental carcinogenicity data and 37 descriptors taking into account size, shape, electronic structure and hydrophobicity of the molecules was analysed with the SVM and ANN. The architecture of the ANN is a fully connected three-layer design with the error-back-propagation algorithm. For both methods, models were optimized using a cross-validation test for the training dataset, and their performances were evaluated using the test dataset. The training of ANNs took several months using seven computers to solve the problems, such as over-training, over-fitting and local minima, while SVM gave a predictability of 74% just comparable with that by ANN, in a much shorter computation time. The prediction accuracy was higher than the best predictability value of 71% reported in the literature for the same dataset (Helma et al, http://www.informatik.uni-freiburg.de/~ml/ptc/).

Conclusions The SVM, a novel machine learning approach, was applied to the structure–carcinogenicity problem based on the information on molecular structure alone. From the analysis of the results obtained, a non-linear model using SVM produced a better model with good predictive ability than the artificial neural network approach. The prediction results were quite good and reasonable under the present uncertainties of the experimental animal carcinogenic data.

Benigni, R. (2003) *Quantitative Structure-Activity Relationship* (*QSAR*) *models of mutagens and carcinogens*. CRC Press
Chen, N. et al (2004) *Support vector machine in chemistry.* World Scientific
Tanabe, K. et al (2005) *J. Ecotech. Res*. **11**: 111–116

87
Novel phenothiaziniums as putative photo-antiviral agents

M. Wainwright, A. Styles and A. Smith

School of Pharmacy and Chemistry, Liverpool John Moores University, Liverpool, UK.
E-mail: m.wainwright@ljmu.ac.uk

Objectives The use of photosensitizers in viral eradication, for example as a topical treatment, or in the disinfection of blood products, has been a clinical reality for over 10 years. However, the efficacy of the photosensitizers employed is less than optimal, usually from the point of view of viral targeting (Wainwright 2005). Methylene blue (MB) is a standard photosensitizer currently employed in viral eradication in blood plasma. The aim of this work was firstly to synthesize novel MB derivatives having one of the original dialkylamino groups replaced by a side chain containing an aromatic ring, and secondly to examine the effect of this substitution on the photosensitizing behaviour and DNA-targeting of the resulting compounds. Substitution patterns in the aromatic side chain were chosen to allow an investigation of any electronic effects on activity and photoproperties.

Methods Phenothiazinium tetraiodide was treated with either diethylamine or di-*n*-propylamine in methanol to furnish the corresponding 3-*N*,*N*-dialkylamino-phenothiazinium tri-iodide. Further reaction with benzylamine derivatives produced the target 3-*N*,*N*-dialkylamino-7-(subs)benzylaminophenothiazinium iodides. Singlet oxygen generation on illumination, and DNA-intercalating activity of the compounds, were carried out spectrophotometrically, relative to the standard photosensitizer MB.

Results Ten new derivatives were obtained by the above procedure, pure chromatography/mass spectrometry. The compounds exhibited intense light absorption in the long-wavelength red region (≈650 nm), which would allow their use in red blood cell fractions or whole blood samples (i.e. at longer wavelengths than haem). Each derivative was shown to produce singlet oxygen in similar yield to that of MB under the same conditions. Each derivative also exhibited a large bathochromic shift when mixed with DNA, demonstrating strongly intercalative behaviour, in a similar fashion to that of dimethyl methylene blue (DMMB), which is known to intercalate much more efficiently than MB (Table 1).

Conclusions The novel derivatives satisfied performance criteria regarding long-wavelength light absorption and singlet oxygen production. Significantly increased DNA intercalation suggests that the anti-viral activities may be higher than that of MB and these are now undergoing cellular testing.

Table 1 Photoproperties and DNA binding of the derivatives

Derivative	Relative yield of $^1O_2$	λ_{max} (H_2O, nm)	λ_{max} + DNA (H_2O, nm)	Shift (nm)
MB (NMe_2/NMe_2)	1.00	665	669	+4
DMMB (NMe_2/NMe_2)	0.55	647	661	+14
$NEt_2/NHCH_2Ph$	0.69	652	666	+14
$NEt_2/NHCH_2(4\text{-}C_6H_4Cl)$	0.71	650	662	+12
$NEt_2/NHCH_2(4\text{-}C_6H_4F)$	0.53	653	665	+12
$NEt_2/NHCH_2(4\text{-}C_6H_4OMe)$	0.54	654	665	+11
$NEt_2/NHCH_2(4\text{-}C_6H_4Me)$	0.57	645	659	+14
$NPr^n_2/NHCH_2Ph$	0.47	658	670	+12
$NPr^n_2/NHCH_2(4\text{-}C_6H_4Cl)$	1.23	656	669	+13
$NPr^n_2/NHCH_2(4\text{-}C_6H_4F)$	0.46	656	666	+10
$NPr^n_2/NHCH_2(4\text{-}C_6H_4OMe)$	0.90	658	669	+11
$NPr^n_2/NHCH_2(4\text{-}C_6H_4Me)$	0.38	658	668	+10

Wainwright, M. (2005) *Photodiag. Photodyn. Ther.* **2**: 263–272

88
Molecular modelling of a lipid bilayer and the use of the bilayer in the rationalization of a small range of percutaneous enhancers

S. Soltani-Khankandani, C. P. Owen and S. Ahmed

Department of Pharmacy, Kingston University, Kingston-upon-Thames, UK.
E-mail: s.ahmed@kingston.ac.uk

Objectives The lipid bilayer represents the most important barrier to molecules entering or leaving a cell. Furthermore, the epidermal structure (in particular the intercellular space) in the skin is also made up of similar bilayer structures which have been under extensive investigation in an attempt to enhance percutaneous absorption by drug substances through the use of skin-penetration enhancers. The ability to formulate compounds which disrupt the barrier and hence enhance the